I&EC research
Industrial & Engineering Chemistry Research
pubs.acs.org/IECR
Article

Binary Blends Versus Ternary Blends in Steam Cogasification by Means of TGA–MS: Reactivity and H_2/CO Ratio

María Puig-Gamero, Ángel Alcazar-Ruiz, Paula Sánchez, and Luz Sanchez-Silva*

Cite This: *Ind. Eng. Chem. Res.* 2020, 59, 12801–12811
Read Online

ACCESS | Metrics & More | Article Recommendations

ABSTRACT: Cogasification of olive pomace, almond shell, and petcoke was carried out by thermogravimetric analysis coupled with mass spectrometry. Binary and ternary blends were compared in terms of their reactivity, outlet-gas emissions, H_2/CO ratios of effluents, and synergistic effect. Synergistic and antagonistic effects were observed with cogasification of blends, but that depended on the ratios of raw materials in the feed. In this regard, the higher the biomass content, the greater the weight loss, the higher the decomposition rate and, thus, the higher the gasification reactivity. Moreover, the synergistic effect on the gasification of the raw materials did not show a clear trend in gas emissions. In general, the higher the biomass content, the greater the H_2 and CO_2 yields, and the less CO was released. On comparing binary and ternary blends, it was seen that the former presented better results in most parameters studied.

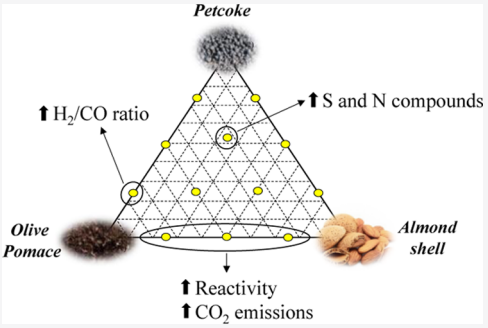

Downloaded via UNIV DE CASTILLA LA MANCHA on May 5, 2022 at 10:50:16 (UTC).
See https://pubs.acs.org/sharingguidelines for options on how to legitimately share published articles.

1. INTRODUCTION

Despite the current trend toward adopting sustainable energy sources in order to reduce greenhouse gas emissions, world's energy is still largely produced by fossil fuels whose consumption is still increasing. According to the 2018 BP statistical review of world energy, total primary energy consumption amounted to 13.5 billion tonnes of oil equivalent in 2017,[1] with 85% of total energy sourced from fossil resources. Simultaneously, petroleum coke or petcoke (PC, a refinery byproduct) production has increased.[2] PC consists of polycyclic aromatic hydrocarbons with high carbon content. It has a high calorific value and availability, low ash and hydrogen content, and is economical. However, one of its main drawbacks is its high sulfur content. Steam gasification is the most efficient way of using petcoke as it reduces emissions of pollutants into the air.[3] In addition, steam gasification is considered to be one of the most effective and efficient techniques for generating hydrogen and electric power. Moreover, the gas product from gasification, syngas, can be also used in the Fischer–Tropsch synthesis that yields liquid fuels. However, its high C/H ratio, low amount of volatiles and, in turn, low gasification reactivity have restricted its use in the gasification industry.[4]

Moreover, biomass gasification has been lauded as the most viable option for a sustainable future by replacing fossil fuels. In addition, efficient use of biomass energy resources can provide employment opportunities, environmental benefits, and improve the rural infrastructure. In this regard, waste from olives and almonds is viable as a fuel, as olive oil production is one of the most important economic activities in Spain, with an annual global production of 2.9 million tons of end product.[5] However, in the production process, large amounts of waste are generated, namely olive pomace, which is a slurry mainly composed of water, flesh, and olive stone. Olive trees (1 ha) can produce 534 kg of dry olive pomace (data from Aceites García de la Cruz oil mill). Also, demand for almonds has increased in Spain, as it has a climate favorable to production, and it is the third largest almond producer in the world after USA and Australia. The current national production average for almond shells and almond grains per annum is approximately 200,0000 and 50,000 tons, respectively. Thus, the main residue is the shell, which can represent up to 70 wt % of total weight.[6] Moreover, at present, renewable chemical industries have shown tremendous interest in it from both an economical and environmental perspective because it provides an alternative to fossil fuels. However, biomass gasification has not been fully industrialized as it has a lower calorific value and energy density, higher tar yield, unreliable supply, and is heterogeneous as a raw material.[7] In this respect, cogasification of petcoke, olive pomace, and almond shell is one possible alternative to solving problems associated with gasifying each of them separately. Moreover, the high volatile matter (VM) present in biomass and the high fixed carbon content in petcoke make cogasification an attractive option as it yields

Received: March 18, 2020
Revised: June 12, 2020
Accepted: June 18, 2020
Published: June 29, 2020

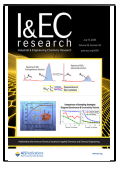

© 2020 American Chemical Society

https://dx.doi.org/10.1021/acs.iecr.0c01399
Ind. Eng. Chem. Res. 2020, 59, 12801–12811

Table 1. Ultimate Analysis, Proximate Analysis, Mineral Content, and HHV of the Petcoke, Almond Shell, and Olive Pomace samples[a]

	proximate analysis (wt %)*daf				ultimate analysis (wt %)*daf				
	moisture	ash	volatile matter	fixed carbon*diff	C	H	N	O*diff	S
petcoke	7.00	0.26	13.00	79.74	82.21	3.11	1.90	7.02	5.50
almond shell	3.97	3.72	73.00	19.31	43.04	5.58	0.72	50.66	nd
olive pomace	2.12	7.77	80.73	9.38	52.49	6.66	1.51	31.31	0.26

	mineral content (ppm)								
	Al	Ca	Fe	K	Mg	Na	Zn	Si	Ti
petcoke	1982		840			158		99311	100
almond shell				54270	262	3305			
olive pomace		2995		23005	515			100288	31

	HHV (MJ/kg)
petcoke	32.2
almond shell	16.3
olive pomace	22.8

[a]*daf: dry and ash-free basis; O^diff: % of oxygen calculated from difference of C, H, N, and S; Fixed carbon*diff: % of fixed carbon was calculated from difference in moisture, ash, and volatile matter; nd: non detectable.

high-quality syngas. In addition, cogasification of different types of feedstocks can produce synergistic effects during the process, thereby further improving gas yield and quality.[8]

Therefore, there can be no doubt that cogasification must be researched in the laboratory before carrying it out on an industrial scale. For this purpose, the thermogravimetric and mass spectrometry analysis (TGA−MS) has proven to be a powerful tool for researching thermochemical conversion of biomass in order to make an initial assessment before scaling-up.[9−11] As a result, Jayaraman et al. studied the gasification characteristics of petcoke and coal−petcoke mixtures with TGA−MS.[10] The gasification reactivity from copyrolysis of coal and corn stalks char was studied with TGA. In addition, the influence of copyrolysis on cogasification reactivity was quantitatively characterized with the synergy index by Chen et al.[12] In addition, Zhu et al., researched cogasification of beech wood and polyethylene in a fluidized-bed reactor.[13] Different ratios of spirit-based distillers' grains and anthracite coal with cogasification were researched by Lv et al.[14] Nevertheless, most studies to date have focused on cogasification of binary blends, and there has been little research on the differences between binary and ternary blends in the steam cogasification of three different raw materials. For this reason, in this paper, cogasification of binary and ternary blends of olive pomace, almond shell, and petcoke was compared in terms of their reactivity, outlet-gas emissions, H_2/CO ratios of effluents, and synergistic effect with the TGA−MS analysis.

2. MATERIALS AND METHODS

2.1. Materials. Olive pomace obtained from "Aceites Garcia de la Cruz" olive oil mill, Madridejos (Toledo, Spain), almond shell obtained from Castilla La Mancha region (Spain), and petcoke obtained from a refinery in Puertollano (Ciudad Real, Spain) were the three raw materials used in this research.

Table 1 shows the ultimate analysis, proximate analysis, the metal content, and the higher heating value (HHV) of the three raw materials. The ultimate and proximate analyses were carried out according to standards UNE 15104:2011, UNE-EN ISO18123, UNE 32-004-84, and UNE 32002-95 while the metal content in the samples was determined by inductively coupled plasma spectrometry (ICP). The HHV was determined using a correlation based on the elemental analysis proposed by Channiwala and Parikh.[15]

$$\mathrm{HHV\ (MJ/kg)} = 0.3491\mathrm{C} + 1.1783\mathrm{H} + 0.1005\mathrm{S} - 0.1034\mathrm{O} - 0.0151\mathrm{N} - 0.0211\mathrm{A} \quad (1)$$

where C, H, O, N, S, and A represent the percentage of carbon, hydrogen, oxygen, nitrogen, sulfur, and ash contents on dry basis.

2.2. Equipment and Procedures. *2.2.1. TGA−MS Analysis.* Steam cogasification was performed in a TGA apparatus (TGA−DSC 1, METTLER TOLEDO) coupled with a mass spectrometer (ThermoStar-GSD 320/quadrupole mass analyzer; Pfeiffer Vacuum). The experimental setup used for the gasification experiments was described in a previous study.[9]

Cogasification was carried out in three different steps:

1. The sample was dried at 105 °C.
2. Pyrolysis was performed at temperatures ranging from 105 to 1000 °C with a heating rate of 40 °C/min and a constant flow of 200 NmL/min in an Ar atmosphere.
3. Steam gasification was carried out at 900 °C for 120 min. Steam was generated in a bubbler system. Ar (50 NmL/min) was constantly bubbled through degassed water heated to 33 °C. The Ar−H_20 mixture was assumed to be saturated, and a gas stream of 5 vol % water in Ar was obtained.

Previous studies were carried out according to the procedure described by Sanchez-Silva et al.[9] for both pyrolysis and gasification in order to avoid the effects of heat and mass transfer limitations. The initial sample weight was fixed at 20 mg. First, the raw materials were oven-dried for 5 h, milled, and sieved to an average particle size of 100−150 μm. The blends of raw materials were then physically mixed, and 1 g of each blend was prepared to ensure homogeneity. Table 2 shows the composition of the blends prepared and their denominations for identification purposes.

Each sample was analyzed at least three times, and average values were recorded. The experimental standard deviation was ±0.5% in weight loss and ±2 °C in temperature. Finally, the gas produced during cogasification was analyzed by means of a

https://dx.doi.org/10.1021/acs.iecr.0c01399
Ind. Eng. Chem. Res. 2020, 59, 12801−12811

Table 2. Olive Pomace/Almond Shell/Petcoke Ratio Used in the Different Blends

sample	petcoke (wt %)	olive pomace (wt %)	almond shell (wt %)
petcoke (P)	100	0	0
olive pomace (op)	0	100	0
almond shell (A)	0	0	100
0P25op75A	0	25	75
0P50op50A	0	50	50
0P75op25A	0	75	25
25P0op75A	25	0	75
50P0op50A	50	0	50
75P0op25A	75	0	25
50P50op0A	50	50	0
25P75op0A	25	75	0
75P25op0A	75	25	0
25P25op50A	25	25	50
25P50op25A	25	50	25
50P25op25A	50	25	25

mass spectrometer (ThermoStar-GSD 320/quadrupole mass analyzer; Pfeiffer Vacuum).

2.2.2. Char Reactivity. Char reactivity was calculated with the following equation

$$R_i = -\frac{1}{w_i}\cdot\frac{dw}{dt} = \frac{1}{1-x_i}\cdot\frac{dx_i}{dt} \quad (2)$$

where x_i and w_i represent the conversion and weight of char at any given time, respectively. Char reactivity, which depends on temperature and gas composition, describes the conversion trend throughout gasification. In this paper, reactivity at 50% (R_{50}) and at 90% (R_{90}) of char conversion was considered for comparative purposes.[16−20]

3. RESULTS AND DISCUSSION

First, there was a physicochemical analysis of the raw materials used in this research. Table 1 shows the ultimate and proximate analyses of almond shell, olive pomace, and petcoke. Regarding the proximate analysis, the biomasses had higher VM, ash content, lower fixed carbon, and moisture than petcoke, as expected. In general, a high volatile content is linked to high reactivity.[19] In addition, the petcoke had higher contents of C, N, and S than did olive pomace and almond shell (Table 1). The high amount of C in the raw materials may increase production of oxygenated species such as CO and CO_2,[21] and nitrogen and sulfur compounds meant there it was more likely that nitrogen (NO_x) and sulfur (SO_x) oxides would be given off due to thermochemical transformation. Furthermore, higher O/C molar ratio values in a fuel lead to

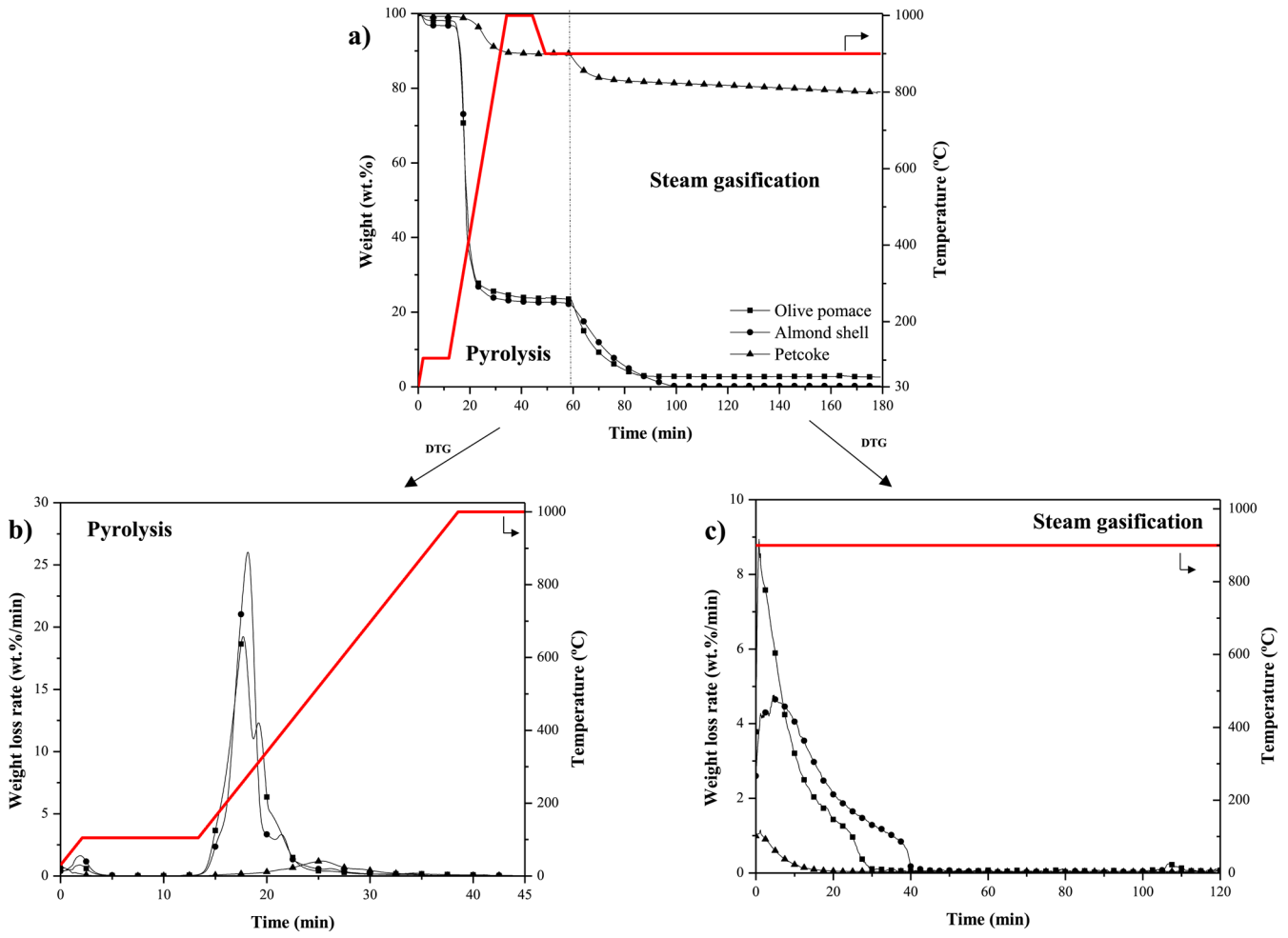

Figure 1. TGA and DTG curves for the pyrolysis and gasification of petcoke, olive pomace, and almond shell; (a) TGA curves for pyrolysis and gasification, (b) DTG curves for pyrolysis, and (c) DTG curves for gasification.

https://dx.doi.org/10.1021/acs.iecr.0c01399
Ind. Eng. Chem. Res. 2020, 59, 12801−12811

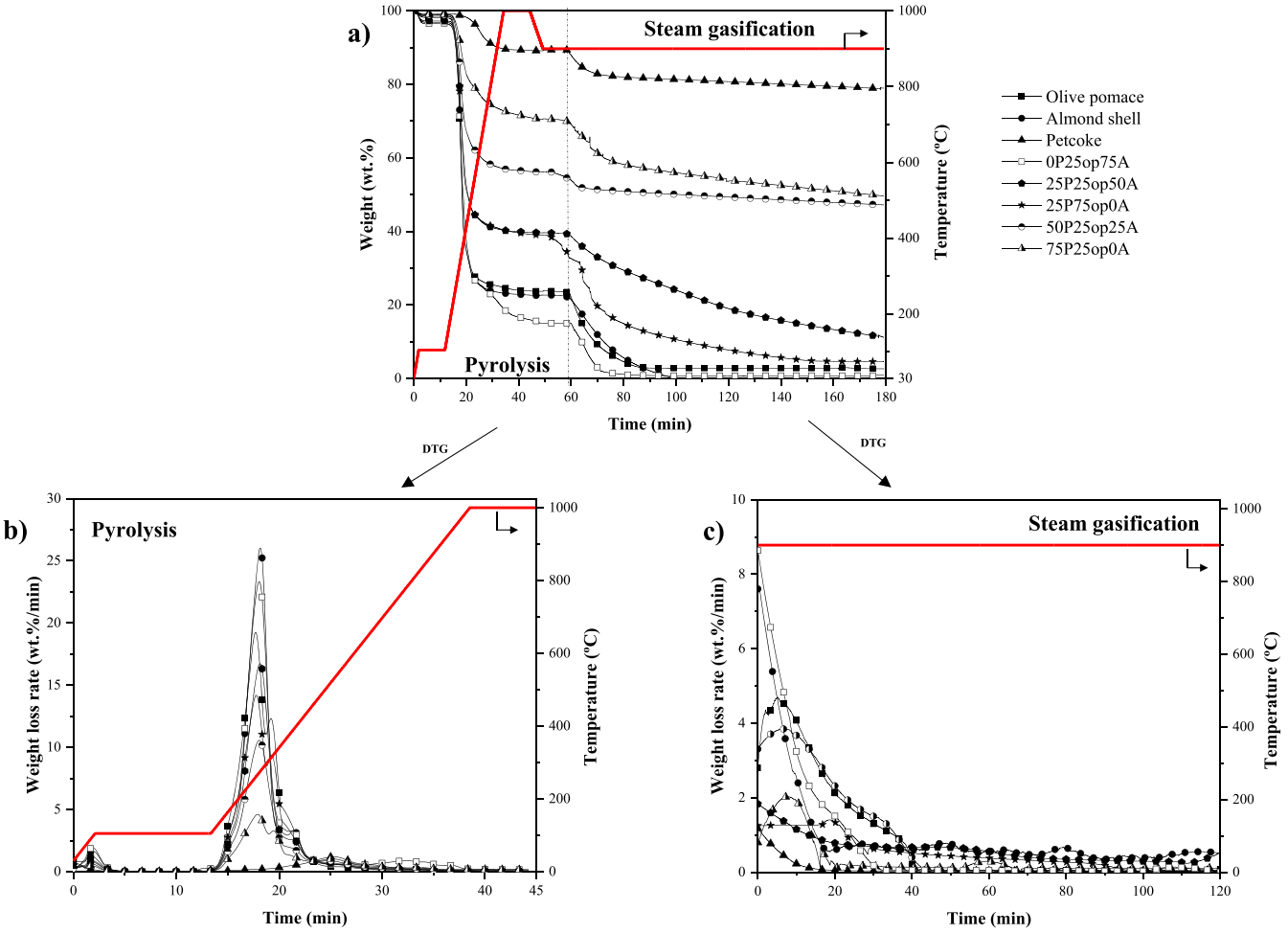

Figure 2. TGA and DTG curves for copyrolysis and cogasification of petcoke, olive pomace, and almond shell; (a) TGA curves for copyrolysis and cogasification, (b) DTG curves for copyrolysis, and (c) DTG curves for cogasification.

Table 3. Pyrolysis Characteristics for Petcoke, Almond Shell, and Olive Pomace

sample	T_m [a] (°C)	$(dw/dt)_{max}$ (wt %/°C) [b]	char yield (wt %)
petcoke	532	1.2	89.6
olive pomace	260	19.3	23.6
almond shell	276	26.0	22.6
0P25op75A	275	23.2	15.0
0P50op50A	265	21.8	22.6
0P75op25A	260	20.7	21.9
25P0op75A	277	13.2	38.6
25P25op50A	273	16.7	39.6
25P50op25A	265	17.9	40.7
25P75op0A	262	14.2	38.8
50P0op50A	279	12.7	54.6
50P25op25A	274	10.5	56.4
50P50op0A	264	9.2	57.2
75P0op25A	279	6.4	72.4
75P25op0A	267	4.6	70.2

[a]Temperature at which a maximum peak in the DTG curve was observed. [b]Maximum decomposition rate.

Table 4. Gasification Characteristics for Petcoke, Olive Pomace, Almond Shell, and Their Blends

sample	R_{50} (1/min)	t_{50} (min)	R_{90} (1/min)	t_{90} (min)
petcoke	0.074	7.07	0.031	86.17
olive pomace	0.128	6.53	0.155	20.32
almond shell	0.073	11.80	0.135	29.77
0P25op75A	0.128	4.25	0.735	10.78
0P50op50A	0.069	13.18	0.155	30.67
0P75op25A	0.108	6.40	0.201	19.23
25P0op75A	0.031	18.45	0.035	81.82
25P25op50A	0.018	36.48	0.044	95.13
25P50op25A	0.027	24.83	0.039	87.52
25P75op0A	0.034	12.35	0.031	63.58
50P0op50A	0.011	29.77	0.049	99.05
50P25op25A	0.008	23.20	0.046	99.67
50P50op0A	0.017	41.57	0.052	101.82
75P0op25A	0.039	18.30	0.036	91.03
75P25op0A	0.042	14.43	0.045	92.80

a fall in its calorific value. The molar ratios for almond shell, olive pomace, and petcoke were 0.883, 0.447, and 0.064, respectively. The H/C molar ratio values were 1.556, 4.523, and 0.453 for almond shell, olive pomace, and petcoke, respectively. Finally, Table 1 lists the mineral content in the different raw materials. In previous research, alkali and alkaline earth metals were observed to reduce the operating temperature of the process.[10,22] In this regard, almond shell and olive pomace contained a high concentration of alkali and alkaline earth elements as calcium (Ca), potassium (K), magnesium (Mg), or sodium (Na).[23,24] These elements may have acted as

https://dx.doi.org/10.1021/acs.iecr.0c01399
Ind. Eng. Chem. Res. 2020, 59, 12801−12811

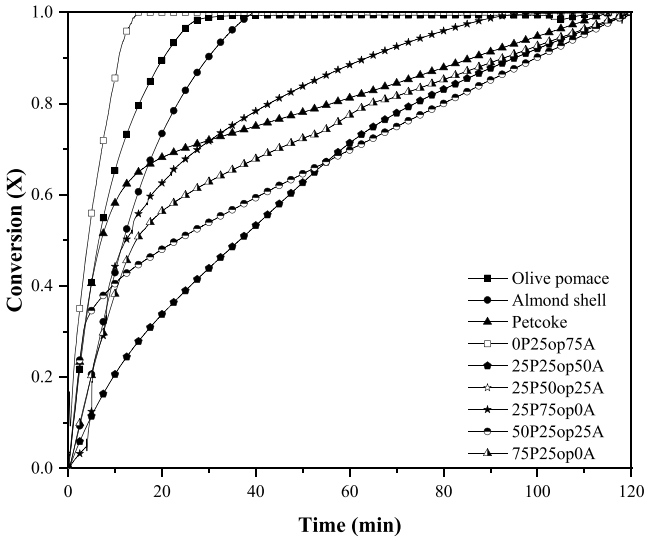

Figure 3. Evolution of char conversion from petcoke, olive pomace, almond shell, and their blends over time.

catalysts, which could favor reactivity and heterogeneous gasification of the char produced.[21] In addition, Na and K can react with CO and CO_2 to produce carbonate and thus reduce the amount of these emissions in the resulting gas.[25] Similarly, these metals can form sulfates and nitrates, reducing the nitrogen and sulfur compound emissions. Furthermore, the fast diffusion of K and Na through the carbon matrix can lead to micropore or mesopore formation, which increases the reaction rate.[26] In addition, Na can catalyze the water-gas shift reaction and promote tar cracking, facilitating the production of H_2.[27] Regarding temperature gasification, temperatures in the range of 750−950 °C can favor the catalyst effect of K.[28] Concerning Ca, its activity decreases at higher conversions; in addition, it can be deactivated by sintering.[28] Nevertheless, interest in calcium-catalyzed gasification remains because it can be used as a sorbent to remove the CO_2, and thus, increasing the heating value of the produced syngas.[29] Moreover, there was a high amount of alumina (Al) and silica (Si) in the petcoke. These elements can promote the deactivation of K and Na as catalysts. They react with Al and Si to form stable and unreactive aluminosilicates at high temperatures (1000−1100 °C),[30] causing inhibition of the gasification reaction.[31] However, when the K amount and the K/Al ratio in the blend increased by addition of biomass to petcoke, petcoke gasification can be enhanced.[31]

3.1. TGA of Pyrolysis and Gasification of Raw Materials. Figure 1 shows the TGA/derivative thermogravimetry (DTG) profiles for pyrolysis and gasification of three raw materials (almond shell, olive pomace, and petcoke). The main pyrolysis step for biomass took place at temperatures between 120 and 450 °C, as can be seen from their DTG profile in Figure 1b. However, the main stage of petcoke pyrolysis occurred from 250 to 850 °C. The pyrolysis was divided into three common degradation stages:[32,33] drying, devolatilization, and char formation. For biomass, a shoulder was observed at temperatures around 300 °C, which was attributed to hemicellulose decomposition. The shoulder was steeper for the almond shell sample, which has been a result of its higher hemicellulose content.[16] Then, the maximum weight loss rate was observed at 400 °C for the almond shell and olive pomace. This shoulder was associated with cellulose decomposition. At this stage, the almond shell and olive pomace samples showed similar weight losses, which can be indicative of similar cellulose content. However, a small peak was observed for olive pomace, which may be because of lipid decomposition from the olive oil it contains.[34] Finally, the highest peak was followed by a tail, which was ascribed to lignin decomposition, which leads to char formation. Olive pomace and almond shell had similar char yields, which could be a result of their similar lignin content. As for petcoke, it had lower weight loss and a higher decomposition temperature than olive pomace and almond shell, as expected. These results were related to the large amount of VM and high concentration of alkali and alkaline earth elements in the biomass (Table 1). The petcoke sample showed the highest weight loss at 550−700 °C, which corresponded to devolatilization. Moreover, it had the highest char yield (89.6 wt %), which indicated that petcoke was more thermally stable than biomass. These results concur well with those reported by Puig-Gamero et al.[7]

Figure 1c shows the DTG profiles for steam gasification of the char produced from three raw materials (almond shell, olive pomace, and petcoke). Note that gasification of biomass char started as soon as the gasifying agent reached the surface of the char particle. As expected, biomass produced the most reactive char, especially that from olive pomace. The olive pomace and almond shell took around 30 and 40 min, respectively, to be totally gasified, whereas the char produced from the petcoke sample decomposed at a lower rate (>120 min). This was attributed to the low reactivity of petcoke because of its aromatic nature and high heavy aromatic to aliphatic ratio. The aliphatic carbon species present in biomass have relatively weak bonds in comparison with the strong ones of the aromatic compounds present in petcoke, the latter being more heat resistant2. In addition, petcoke gasification was compared with results from a previous study, 18 in which petcoke was gasified at 900 °C for 60 min. The results of gasification conversion were similar to those obtained here at 900 °C for 120 min. In conclusion, there was no improvement with an increase in time for petcoke gasification, which could indicate that steam was insufficient for a complete petcoke gasification.[35]

3.2. TGA of Binary and Ternary Blends during Copyrolysis and Cogasification. In order to study and compare interactions between raw materials during gasification, binary and ternary blends were analyzed. Figure 2 shows the TGA/DTG profiles for steam copyrolysis and cogasification of the blends. In general, the samples had an intermediate trend between the raw materials. Thus, the higher the petcoke content, the higher the char yield. However, gasification of this char was less efficient because of its low reactivity. In this respect, petcoke gasification was improved on blending with biomass. In addition, weight losses for the binary blends of olive pomace and almond shell (samples 0P25op75A and 0P75op25A) were higher than in their raw materials. This can be ascribed to the high amount of K, Na, and Ca in them (Table 1), which acted as catalysts, thereby accelerating the decomposition process.[21]

Figure 2b shows the DTG profile for copyrolysis of raw materials, and Table 3 summarizes the most relevant pyrolysis characteristics of petcoke, almond shell, and olive pomace and their blends. Generally, the higher the biomass content, the higher the weight loss and the higher the decomposition rate. In addition, lower temperatures and times were required,

https://dx.doi.org/10.1021/acs.iecr.0c01399
Ind. Eng. Chem. Res. 2020, 59, 12801−12811

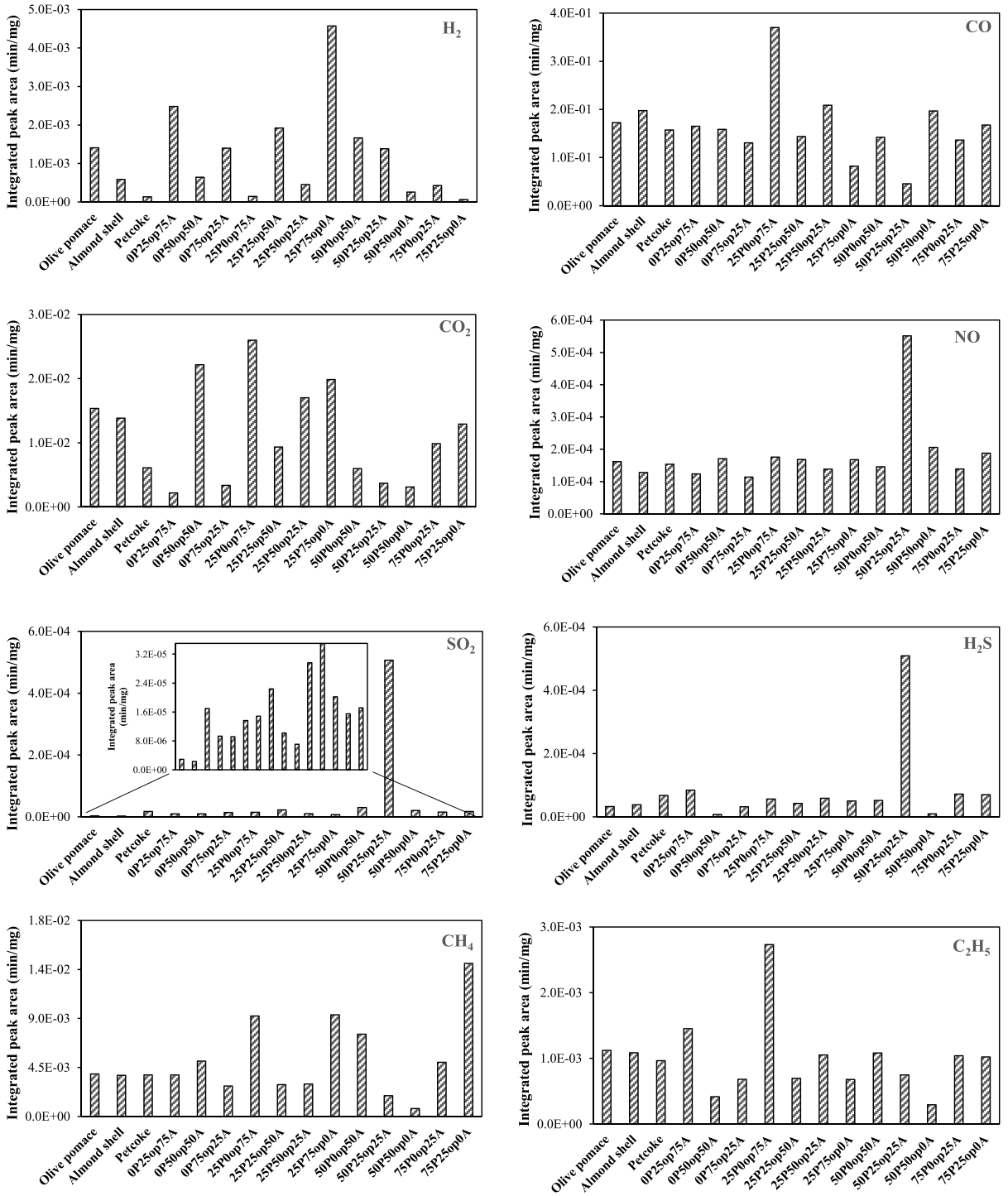

Figure 4. Main gaseous products formed during gasification of olive pomace, almond shell, petcoke, and their blends.

which was because of the high VM content of biomass (Table 1).

Moreover, the DTG profiles for binary and ternary blends were similar and between those for the raw materials. Only, binary samples 0P25op75A and 0P75op25A did not show an intermediate trend, and their degradation rates were higher than those for their raw materials (Table 3). As mentioned above, this was linked to the synergetic effect between them because of their VM content and elemental composition.

Figure 2c shows the DTG curves for steam cogasification of the char produced from copyrolysis. Char gasification also started as soon as the gasifying agent reached the surface of the char particle. Just like what happened in copyrolysis, the weight loss rates for the binary and ternary blends were lower than those for olive pomace and almond shell but higher than that for the petcoke sample in cogasification. Only the binary blends of olive pomace and almond shell showed higher rates than those for their raw materials, which was a direct result of the biomass composition. Finally, the higher the petcoke content, the higher the residue there was for both binary and ternary blends.

https://dx.doi.org/10.1021/acs.iecr.0c01399
Ind. Eng. Chem. Res. 2020, 59, 12801−12811

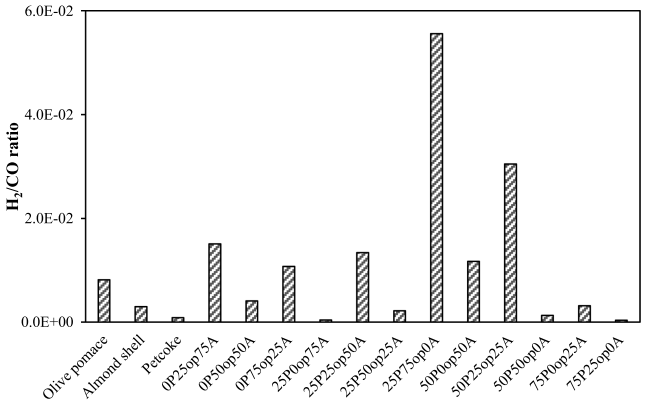

Figure 5. H_2/CO ratio of the gas product during cogasification for olive pomace, almond shell, petcoke, and their blends.

3.3. Reactivity and Char Conversion during Cogasification. Table 4 lists the reactivity parameter at 50% (R_{50}) and 90% (R_{90}) of char conversion and the time required to achieve this conversion (t_{50} and t_{90}) for all samples. Figure 3 shows the char conversion obtained from gasification of all the samples analyzed. Olive pomace had the highest reactivity value and the shortest total gasification time, as it had the greatest amount of VM. Additionally, almond shell and petcoke had similar R_{50} values, but different times were required. However, almond shell reactivity improved as the reaction progressed, although the opposite was observed for petcoke. These results were coherent with the lower weight loss rate for petcoke during gasification.

In general, the higher the degree of conversion, the higher the reactivity, which was because of the mineral content of the raw materials. Alkali and alkaline earth metals captured within the carbon structure are continuously released during devolatilization, and as this is continuous, alkalis become more concentrated in the solid phase, which leads to a higher number of active sites of carbon. Thus, reactivity accelerates as the reaction proceeds.[36] Only with petcoke, reactivity at a 90% conversion was worse than R_{50}, which was attributed to mineral contents inhibiting the process by means of sintering.[36] These results concurred well with the high Al and Si content (Table 1) in the petcoke.

For the binary and ternary blends, the higher the biomass content, the higher the reactivity. It must be stressed that samples 0P25op75A and 0P75op25A had a higher decomposition rate during gasification than their raw materials. However, their reactivity, at 50% of conversion, was lower than that for their raw materials. Nevertheless, as gasification went underway, reactivity for these blends improved in respect to their raw materials. This may be associated with synergistic effects, which will be explained later on. Similarly, sample 50P25op25A had the lowest R_{50} value, although this increased considerably as the process got underway, after which it had a R_{90} value similar to that seen in the other samples. According to these results, the binary blends had better R_{50} and R_{90} values and lower times than ternary blends.

3.4. Evolved Gas Analysis during Cogasification. Figure 4 plots the gas yields calculated by integrating the data measured using MS in the gasification of almond shell, olive pomace, petcoke, and their blends. H_2, CO, CO_2, and CH_4 were the main gases obtained throughout the whole process.

Olive pomace had the highest H_2 yield and CO_2 emissions followed by almond shell and petcoke, which correlated well with the elemental analysis (Table 1). However, the highest CO yield was obtained by almond shell and olive pomace, which can be attributed to their higher potassium content.[37] The high amount of CO obtained indicates that the char gasification (water−gas) reaction ($C + H_2O \rightleftarrows CO + H_2$) and the Boudouard reaction ($C + CO_2 \rightleftarrows 2CO$) predominated. Apart from H_2, CO, and CO_2, light hydrocarbons such as CH_4 and C_2H_2 were obtained in high proportions. Thus, secondary reactions such as thermal cracking and methanization ($C_nH_m \rightleftarrows C_{n-x}H_{m-y} + H_2 + CH_4 + C$; $C + 2H_2 \rightleftarrows CH_4$) took place.[38] The three raw materials had similar yields of CH_4. As for the biomass, this could be explained by the high potassium content in the sample, which was reported in the bibliography as being an active catalyst for methanation.[39] In addition, the high gasification temperature (900 °C) favored the Boudouard reaction, water−gas, and steam−methane reforming, as they are endothermic reactions. Thus, H_2 and CO should have been greater than CH_4 and CO_2.[40,41] However, H_2 production was lower, which may have been because of insufficient steam in gasification, which was conducive to the reverse water-gas shift and steam-reforming reactions.[41] Nitrogen and sulfur compounds were also detected in all samples. These compounds could have originated from water dissociation on the char surface into hydrogen atoms and a hydroxyl radical, which is a highly active oxidizing agent.[42]

Regarding the binary and ternary blends, their gas emissions did not follow any clear trend, which may have been because of the synergistic effect between the raw materials in gasification. In general, the higher the biomass content, particularly olive pomace, the higher the H_2 yield, the higher the CO_2 emissions, and the lower the release of CO. Additionally, CH_4 production was favored when petcoke and olive pomace were gasified together. Finally, emissions of nitrogen and sulfur compounds were higher in the ternary blend, and the highest was seen in sample 50P25op25A.

Figure 5 shows the H_2/CO ratio of the gas product from gasification. This ratio was calculated to determine the synthesis gas quality. As for the raw materials, olive pomace had the highest ratio. However, most blends displayed upper values, the highest of which was for binary sample 25P75op0A, followed by ternary blend 50P25op25A.

3.5. Synergetic Effect Analysis of Olive Pomace, Petcoke, and Almond Shell Blends. The experimental and theoretical data for weight loss (wt %) were compared in order to study the synergistic effects of the ternary and binary blends during cogasification. The theoretical weight loss value (Y_{th}) can be calculated as follows[43]

$$Y_{th} = Y_P \cdot F_P + Y_{op} \cdot F_{op} + Y_A \cdot F_A \quad (3)$$

where F_P, F_{op}, and F_A are the fractions of petcoke, olive pomace, and almond shell in the blends, respectively, and Y_P, Y_{op}, and Y_A are weight losses (wt %) from TGA during cogasification.

The deviation of the experimental and theoretical weight loss (Δy) for the blends can be used to evaluate the synergistic interactions between raw materials. A positive value of Δy indicated that more volatile products could be generated by cogasification than by individual gasification.

$$\Delta y = Y_{th} - Y_{exp} \quad (4)$$

https://dx.doi.org/10.1021/acs.iecr.0c01399
Ind. Eng. Chem. Res. 2020, 59, 12801−12811

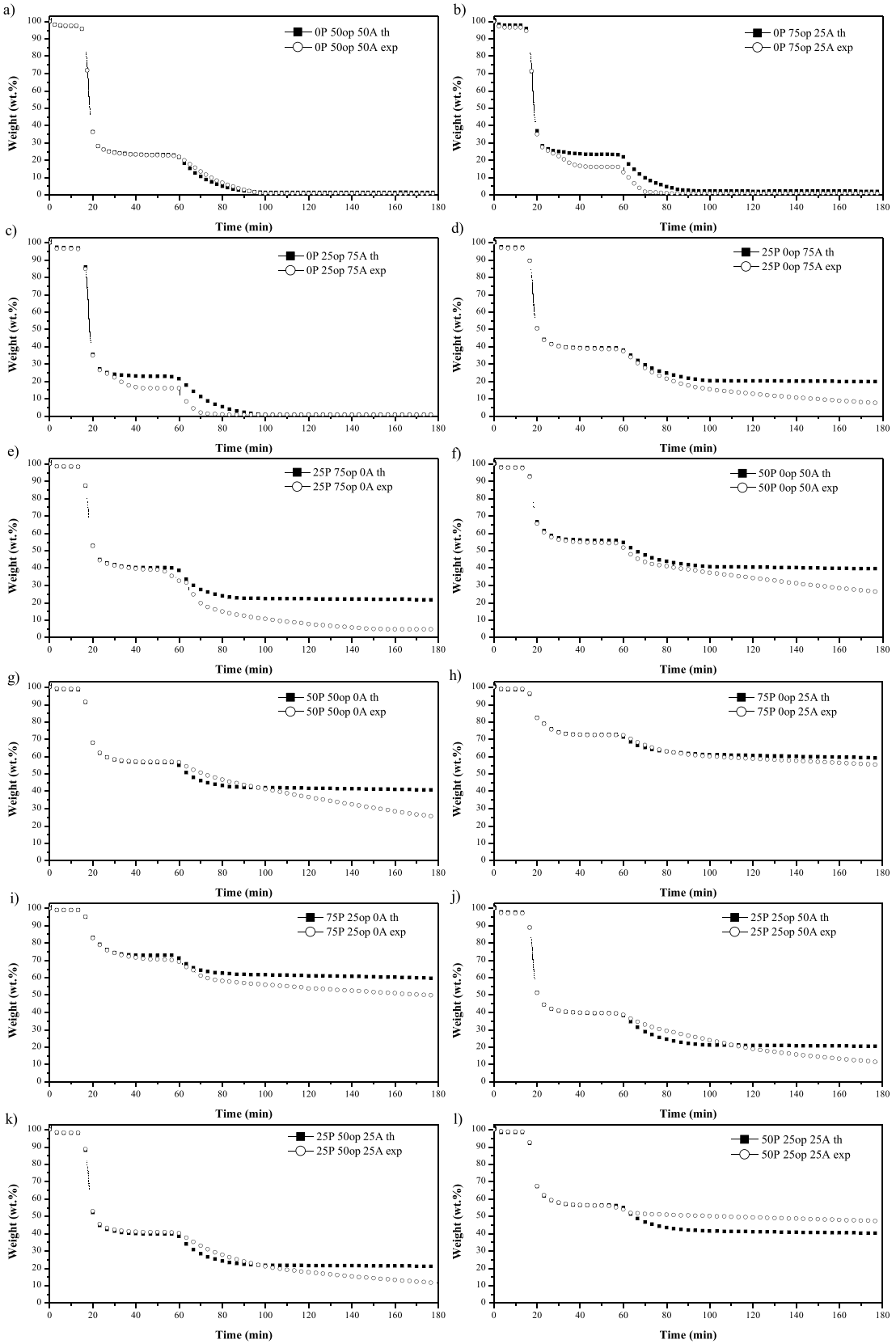

Figure 6. Comparison between experimental and theoretical TGA curves obtained from cogasification of olive pomace, almond shell, and petcoke blends: (a) sample 0P50op50A; (b) sample 0P75op25A; (c) sample 0P25op75A; (d) sample 25P0op75A; (e) sample 25P75op0A; (f) sample 50P0op50A; (g) sample 50P50op0A; (h) sample 75P0op25A; (i) sample 75P25op0A; (j) sample 25P25op50A; (k) sample 25P50op25A; and (l) sample 50P25op25A.

https://dx.doi.org/10.1021/acs.iecr.0c01399
Ind. Eng. Chem. Res. 2020, 59, 12801−12811

where Y_{exp} and Y_{th} are the experimental and theoretical weight loss values, respectively.

Figure 6 compares theoretical and experimental weight losses for each blend. In general, the main differences between the curves were observed in gasification. The physical-chemical properties of the raw materials can explain these differences (Table 1). Regarding the binary blends, samples 0P50op50A and 75P0op25A practically overlapped, and so, any synergistic or antagonistic effects could be discarded. However, a synergistic effect was detected in samples 0P75op25A and 0P25op75A. Weight loss in these samples during pyrolysis was higher, which resulted in less but more reactive char, which, in turn, increased the gasification rate. These results were consistent with reactivity at 50 and 90% of conversion (Table 4), where the reactivity of the blends was higher than that for their raw materials. Once again these findings indicated that the catalytic activity of the inorganic matter in the biomass played a significant role in cogasification.[44−46] Furthermore, the gasification rate for samples 25P0op75A, 75P25op0A, 50P0op50A, and 75P25op0A was higher than expected, which was indicative of a synergetic effect. Moreover, the gasification rate was seen to increase as the process got underway, which was coherent with the increase in reactivity when char conversion also increased (Table 4), as explained previously. Theoretical and experimental data from the TGA curves were also different to sample 50P50op0A. Both curves overlapped during pyrolysis (no synergistic or antagonistic effect). However, the theoretical gasification rate slowly decreased, whereas the experimental one hardly changed, and no maximum was detected. At the early stage of gasification, the experimental data were higher than theoretical ones (antagonistic effect); as the process proceeded, the values from the experimental data were better than the theoretical ones, which may indicate that the mineral content in the different raw materials was acting as a catalyst to gasification (synergetic effect). Moreover, this synergetic effect could be attributed to the high H/C ratio in olive pomace in comparison with petcoke. Thus, olive pomace could quickly decompose to form free radicals, which reacted with the organic matter, thereby promoting decomposition, oxidation, and gasification reactions in the petcoke. This improved the decomposition rate and petcoke gasification.[8] As for the ternary blends, samples 25P25op50A and 25P50op25A behaved similarly to sample 50P50op0A. On a final note, sample 50P25op25A was the only blend with an antagonistic effect throughout the whole gasification process, as weight loss was lower than expected. Thus, in conclusion, the synergistic effect could be said to be more remarkable in the binary blends.

4. CONCLUSIONS

Cogasification of binary and ternary blends of olive pomace, almond shell, and petcoke by TGA−MS was evaluated. The synergistic effect could be observed in both the thermogravimetric and spectrometric analyses during gasification and it depended on the ratios of raw materials. In this regard, the higher the biomass content, the higher the weight loss, the higher the decomposition rate and, thus, the higher the gasification reactivity. As for gas emissions, they did not follow any particular trend, which was a result of the synergistic or antagonistic effect. Additionally, H_2 and CO_2 yields decreased, and CO was increasingly released when petcoke content rose. Finally, thermal treatment of ternary sample 50P25op25A had the highest antagonistic effect, and there were emissions of nitrogen and sulfur compounds. Additionally, binary sample 25P75op0A had the best gas quality in terms of higher H_2/CO ratio and reactivity. Finally, on comparing both binary and ternary blends, in general, the former showed higher reactivity values, a better H_2/CO ratio, a higher synergistic effect, and lower emissions of sulfur and nitrogen compounds.

AUTHOR INFORMATION

Corresponding Author

Luz Sanchez-Silva − *Department of Chemical Engineering, University of Castilla-La Mancha, 13071 Ciudad Real, Spain;* orcid.org/0000-0002-4348-7520; Phone: +34 926 29 53 00 ext. 6307; Email: marialuz.sanchez@uclm.es; Fax: +34 926 29 52 56

Authors

María Puig-Gamero − *Department of Chemical Engineering, University of Castilla-La Mancha, 13071 Ciudad Real, Spain*

Ángel Alcazar-Ruiz − *Department of Chemical Engineering, University of Castilla-La Mancha, 13071 Ciudad Real, Spain*

Paula Sánchez − *Department of Chemical Engineering, University of Castilla-La Mancha, 13071 Ciudad Real, Spain*

Complete contact information is available at: https://pubs.acs.org/10.1021/acs.iecr.0c01399

Notes

The authors declare no competing financial interest.

ACKNOWLEDGMENTS

The authors wish to thank the Spanish government (grant no. FPU15/02653), European Regional Development Fund (TEQUIMA group), and the Regional Government of Castilla-La Mancha (Project SPBLY/17/180501/000238) for their financial support and "Aceites García de la Cruz" olive oil mill.

ABBREVIATIONS

PC	petcoke
op	olive pomace
A	almond shell
VM	volatile matter
TGA	thermogravimetric analysis
DTG	derivative thermogravimetric
MS	mass spectrometry
ICP	inductively coupled plasma spectrometry
R_{50}	reactivity at 50% of char conversion
R_{90}	reactivity at 90% of char conversion

REFERENCES

(1) BP Statistical review of world energy 2.

(2) Okeke, I. J.; Adams, T. A. Combining petroleum coke and natural gas for efficient liquid fuels production. *Energy* **2018**, *163*, 426−442.

(3) Wei, J.; Guo, Q.; Gong, Y.; Ding, L.; Yu, G. Synergistic effect on co-gasification reactivity of biomass-petroleum coke blended char. *Bioresour. Technol.* **2017**, *234*, 33−39.

(4) Wang, G.; Zhang, J.; Huang, X.; Liang, X.; Ning, X.; Li, R. Co-gasification of petroleum coke-biomass blended char with steam at temperatures of 1173−1373 K. *Appl. Therm. Eng.* **2018**, *137*, 678−688.

(5) Cequier, E.; Aguilera, J.; Balcells, M.; Canela-Garayoa, R. Extraction and characterization of lignin from olive pomace: a comparison study among ionic liquid, sulfuric acid, and alkaline treatments. *Biomass Conversi. Biorefin.* **2019**, *9* (2), 241−252.

(6) Liminana, P.; Garcia-Sanoguera, D.; Quiles-Carrillo, L.; Balart, R.; Montanes, N. Optimization of Maleinized Linseed Oil Loading as a Biobased Compatibilizer in Poly(Butylene Succinate) Composites with Almond Shell Flour. *Materials* **2019**, *12*, 685.
(7) Puig-Gamero, M.; Lara-Díaz, J.; Valverde, J. L.; Sánchez, P.; Sanchez-Silva, L. Synergestic effect in the steam co-gasification of olive pomace, coal and petcoke: Thermogravimetric-mass spectrometric analysis. *Energy Convers. Manage.* **2018**, *159*, 140−150.
(8) Yang, Z.; Wu, Y.; Zhang, Z.; Li, H.; Li, X.; Egorov, R. I.; Strizhak, P. A.; Gao, X. Recent advances in co-thermochemical conversions of biomass with fossil fuels focusing on the synergistic effects. *Renew. Sustain. Energy Rev.* **2019**, *103*, 384−398.
(9) Sanchez-Silva, L.; López-González, D.; Garcia-Minguillan, A. M.; Valverde, J. L. Pyrolysis, combustion and gasification characteristics of Nannochloropsis gaditana microalgae. *Bioresour. Technol.* **2013**, *130*, 321−331.
(10) Jayaraman, K.; Gokalp, I. Gasification characteristics of petcoke and coal blended petcoke using thermogravimetry and mass spectrometry analysis. *Appl. Therm. Eng.* **2015**, *80*, 10−19.
(11) Fernandez, A.; Soria, J.; Rodriguez, R.; Baeyens, J.; Mazza, G. Macro-TGA steam-assisted gasification of lignocellulosic wastes. *J. Environ. Manage.* **2019**, *233*, 626−635.
(12) Chen, X.; Liu, L.; Zhang, L.; Zhao, Y.; Qiu, P. Gasification reactivity of co-pyrolysis char from coal blended with corn stalks. *Bioresour. Technol.* **2019**, *279*, 243−251.
(13) Zhu, H. L.; Zhang, Y. S.; Materazzi, M.; Aranda, G.; Brett, D. J. L.; Shearing, P. R.; Manos, G. Co-gasification of beech-wood and polyethylene in a fluidized-bed reactor. *Fuel Process. Technol.* **2019**, *190*, 29−37.
(14) Lv, J.; Ao, X.; Li, Q.; Cao, Y.; Chen, Q.; Xie, Y. Steam co-gasification of different ratios of spirit-based distillers' grains and anthracite coal to produce hydrogen-rich gas. *Bioresour. Technol.* **2019**, *283*, 59−66.
(15) Channiwala, S. A.; Parikh, P. P. A unified correlation for estimating HHV of solid, liquid and gaseous fuels. *Fuel* **2002**, *81*, 1051−1063.
(16) López-González, D.; Fernandez-Lopez, M.; Valverde, J. L.; Sanchez-Silva, L. Gasification of lignocellulosic biomass char obtained from pyrolysis: Kinetic and evolved gas analyses. *Energy* **2014**, *71*, 456−467.
(17) Mandapati, R. N.; Daggupati, S.; Mahajani, S. M.; Aghalayam, P.; Sapru, R. K.; Sharma, R. K.; Ganesh, A. Experiments and kinetic modeling for CO2 gasification of indian coal chars in the context of underground coal gasification. *Ind. Eng. Chem. Res.* **2012**, *51*, 15041−15052.
(18) Gómez-Barea, A.; Ollero, P.; Fernández-Baco, C. Diffusional effects in CO2 gasification experiments with single biomass char particles. 1. Experimental investigation. *Energy Fuels* **2006**, *20*, 2202−2210.
(19) Mitsuoka, K.; Hayashi, S.; Amano, H.; Kayahara, K.; Sasaoaka, E.; Uddin, M. A. Gasification of woody biomass char with CO2: The catalytic effects of K and Ca species on char gasification reactivity. *Fuel Process. Technol.* **2011**, *92*, 26−31.
(20) Zhang, Y.; Hara, S.; Kajitani, S.; Ashizawa, M. Modeling of catalytic gasification kinetics of coal char and carbon. *Fuel* **2010**, *89*, 152−157.
(21) Fermoso, J.; Arias, B.; Gil, M. V.; Plaza, M. G.; Pevida, C.; Pis, J. J.; Rubiera, F. Co-gasification of different rank coals with biomass and petroleum coke in a high-pressure reactor for H2-rich gas production. *Bioresour. Technol.* **2010**, *101*, 3230−3235.
(22) Nemanova, V.; Abedini, A.; Liliedahl, T.; Engvall, K. Co-gasification of petroleum coke and biomass. *Fuel* **2014**, *117*, 870−875.
(23) Zhou, C.; Liu, G.; Wang, X.; Qi, C. Co-combustion of bituminous coal and biomass fuel blends: Thermochemical characterization, potential utilization and environmental advantage. *Bioresour. Technol.* **2016**, *218*, 418−427.
(24) He, Q.; Yu, J.; Song, X.; Ding, L.; Wei, J.; Yu, G. Utilization of biomass ash for upgrading petroleum coke gasification: Effect of soluble and insoluble components. *Energy* **2020**, *192*, 116642.
(25) Gai, C.; Guo, Y.; Liu, T.; Peng, N.; Liu, Z. Hydrogen-rich gas production by steam gasification of hydrochar derived from sewage sludge. *Int. J. Hydrogen Energy* **2016**, *41*, 3363−3372.
(26) Virla, L. D.; Montes, V.; Wu, J.; Ketep, S. F.; Hill, J. M. Synthesis of porous carbon from petroleum coke using steam, potassium and sodium: Combining treatments to create mesoporosity. *Microporous Mesoporous Mater.* **2016**, *234*, 239−247.
(27) Yuan, H.; Wu, S.; Yin, X.; Huang, Y.; Guo, D.; Wu, C. Adjustment of biomass product gas to raise H2/CO ratio and remove tar over sodium titanate catalysts. *Renewable Energy* **2018**, *115*, 288−298.
(28) Arnold, R. A.; Hill, J. M. Catalysts for gasification: a review. *Sustainable Energy Fuels* **2019**, *3*, 656−672.
(29) Parthasarathy, P.; Narayanan, K. S.; Ceylan, S.; Pambudi, N. A. Optimization of Parameters for the Generation of Hydrogen in Combined Slow Pyrolysis and Steam Gasification of Biomass. *Energy Fuels* **2017**, *31*, 13692−13704.
(30) Fan, Y.; Zhang, H.; Lyu, Q.; Zhu, Z. Investigation of slagging characteristics and anti-slagging applications for Indonesian coal gasification. *Fuel* **2020**, *267*, 117285.
(31) Cabuk, B.; Duman, G.; Yanik, J.; Olgun, H. Effect of fuel blend composition on hydrogen yield in co-gasification of coal and non-woody biomass. *Int. J. Hydrogen Energy* **2020**, *45*, 3435−3443.
(32) López-González, D.; Fernandez-Lopez, M.; Valverde, J. L.; Sanchez-Silva, L. Pyrolysis of three different types of microalgae: Kinetic and evolved gas analysis. *Energy* **2014**, *73*, 33−43.
(33) Puig-Gamero, M.; Fernandez-Lopez, M.; Sánchez, P.; Valverde, J. L.; Sanchez-Silva, L. Pyrolysis process using a bench scale high pressure thermobalance. *Fuel Process. Technol.* **2017**, *167*, 345−354.
(34) López-González, D.; Puig-Gamero, M.; Acién, F. G.; García-Cuadra, F.; Valverde, J. L.; Sanchez-Silva, L. Energetic, economic and environmental assessment of the pyrolysis and combustion of microalgae and their oils. *Renew. Sustain. Energy Rev.* **2015**, *51*, 1752−1770.
(35) Krerkkaiwan, S.; Fushimi, C.; Tsutsumi, A.; Kuchonthara, P. Synergetic effect during co-pyrolysis/gasification of biomass and sub-bituminous coal. *Fuel Process. Technol.* **2013**, *115*, 11−18.
(36) Chen, J.; Fan, Y.; E, J.; Cao, W.; Zhang, F.; Gong, J.; Liu, G.; Xu, W. Effects analysis on the gasification kinetic characteristics of food waste in supercritical water. *Fuel* **2019**, *241*, 94−104.
(37) Ong, H. C.; Chen, W.-H.; Farooq, A.; Gan, Y. Y.; Lee, K. T.; Ashokkumar, V. Catalytic thermochemical conversion of biomass for biofuel production: A comprehensive review. *Renew. Sustain. Energy Rev.* **2019**, *113*, 109266.
(38) Widyawati, M.; Church, T. L.; Florin, N. H.; Harris, A. T. Hydrogen synthesis from biomass pyrolysis with in situ carbon dioxide capture using calcium oxide. *Int. J. Hydrogen Energy* **2011**, *36*, 4800−4813.
(39) Nanou, P.; Van Rossum, G.; Van Swaaij, W. P. M.; Kersten, S. R. A. Evaluation of catalytic effects in gasification of biomass at intermediate temperature and pressure. *Energy Fuels* **2011**, *25*, 1242−1253.
(40) Fernandez-Lopez, M.; Pedroche, J.; Valverde, J. L.; Sanchez-Silva, L. Simulation of the gasification of animal wastes in a dual gasifier using Aspen Plus. *Energy Convers. Manage.* **2017**, *140*, 211−217.
(41) Puig-Gamero, M.; Argudo-Santamaria, J.; Valverde, J. L.; Sánchez, P.; Sanchez-Silva, L. Three integrated process simulation using aspen plus: Pine gasification, syngas cleaning and methanol synthesis. *Energy Convers. Manage.* **2018**, *177*, 416−427.
(42) Chaudhari, S. T.; Dalai, A. K.; Bakhshi, N. N. Production of hydrogen and/or syngas (H2 + CO) via steam gasification of biomass-derived chars. *Energy Fuels* **2003**, *17*, 1062−1067.
(43) Zhang, Z.; Pang, S.; Levi, T. Influence of AAEM species in coal and biomass on steam co-gasification of chars of blended coal and biomass. *Renewable Energy* **2017**, *101*, 356−363.
(44) Alvarez, J.; Lopez, G.; Amutio, M.; Bilbao, J.; Olazar, M. Evolution of biomass char features and their role in the reactivity

https://dx.doi.org/10.1021/acs.iecr.0c01399
Ind. Eng. Chem. Res. 2020, 59, 12801−12811

during steam gasification in a conical spouted bed reactor. *Energy Convers. Manage.* **2019**, *181*, 214−222.
(45) Gil, M. V.; Rubiera, F. Coal and biomass cofiring: fundamentals and future trends. In *New Trends in Coal Conversion*; Elsevier, 2019; pp 117−140.
(46) Wu, Z.; Li, Y.; Xu, D.; Meng, H. Co-pyrolysis of lignocellulosic biomass with low-quality coal: optimal design and synergistic effect from gaseous products distribution. *Fuel* **2019**, *236*, 43−54.

https://dx.doi.org/10.1021/acs.iecr.0c01399
Ind. Eng. Chem. Res. 2020, 59, 12801−12811